Short Papers

Full-Wave CAD of a Rectangular Waveguide Filter with Integrated Coaxial Excitation

Giampiero Gerini and Marco Guglielmi

***Abstract*—Coaxial waveguides are very commonly used in many microwave subsystems for the connection of various components. Significant size reduction could, therefore, be achieved by integrating the design of the coaxial transition in the computer-aided design (CAD) of microwave filters. In this context, we first discuss in this paper a coaxial transition, which can be efficiently designed interactively using an accurate and efficient CAD procedure. The key elements of the CAD tool developed are then described and a specific example of a microwave filter is discussed. In addition to theory, measured results are also presented, thereby fully validating both the CAD tool and the structures proposed.**

***Index Terms*—Coaxial waveguides, electromagnetic launching, waveguide excitation, waveguide filters.**

I. Introduction

Microwave passive components are usually designed first with standard waveguide ports, and are then fitted with waveguide-to-coaxial transitions. By integrating the coaxial transition directly in the hardware design, significant savings in size and mass would be achieved. A large number of theoretical contributions can indeed be found in the technical literature for the study of rectangular-waveguide-to-coaxial-waveguide transitions (see, e.g., [1]–[13]). Few of the available results, however, can be used for filter design since they are all essentially concerned with the determination of the input impedance at the coaxial port. More complete and accurate results, which could, in principle, be of use for filter design are also available [14]. The approach in [14], however, requires very complex frequency-dependent calculations so that its usefulness is, in fact, limited. In this paper, we first discuss a coaxial-to-rectangular-waveguide transition, which is amenable to an accurate and efficient full-wave computer-aided design (CAD) procedure. We then describe the key elements required for the implementation of a CAD tool for the full-wave analysis and optimization of a complete filter structure. In addition to theory, measured results are also presented, thereby fully validating at the same time both the structure of the transition and the CAD tool developed.

II. Coaxial-to-Rectangular-Waveguide Transition

The most commonly used coaxial-to-rectangular-waveguide transition uses a probe acting as an exciting dipole. Although this type of transition is very simple to manufacture, its full-wave electromagnetic analysis requires rather complex frequency-dependent calculations [14]. The situation can be dramatically improved if the geometry of the transition is suitably modified. Another possible geometry is the one shown in Fig. 1 [15]. This type of transition can be decomposed into the cascaded connection of uniform waveguides so that the electromagnetic analysis is considerably simplified.

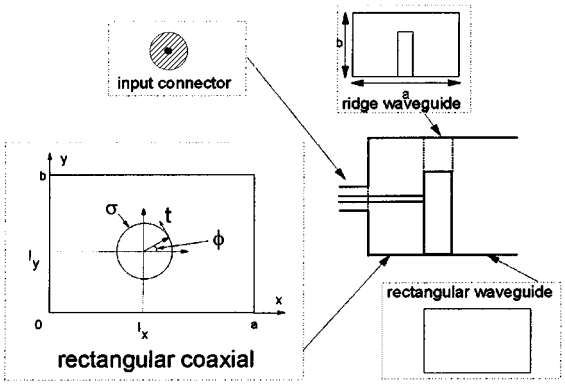

Fig. 1. Collinear coaxial transition in rectangular waveguide.

The analysis approach proposed in [15] is based on the assumption of a given sinusoidal current distribution along the central conductor. The procedure is, therefore, not rigorous and, furthermore, the results obtained are not suitable for integration in a full-wave CAD tool. To obtain a rigorous full-wave result, the structure can indeed be viewed as the cascaded connection of different uniform waveguide sections. However, instead of assuming a given current distribution on the central coaxial conductor, each transition must be analyzed with a full-wave procedure (e.g., [16]). Following this approach, the study of the structure in Fig. 1 is reduced to finding the modes of each uniform waveguide section, and to evaluating the coupling integrals for the modes at the various junctions. The first and last waveguide sections are standard coaxial and rectangular waveguides, respectively. For the remaining two waveguide types, namely, rectangular coaxial and ridge waveguide, some additional work is required.

A. Modal Analysis

A very efficient procedure for computing large numbers of eigenvalues and eigenfunctions of arbitrary waveguide structures is the one given in [18]. According to [18], the modes of a rectangular waveguide modified or perturbed by an arbitrarily shaped cylindrical conductor, for instance, can be obtained by solving three *frequency-independent* integral equations. This procedure can be used to derive the modes of the two noncanonical waveguides in the proposed structure, namely, the rectangular coaxial and ridged waveguide in Fig. 1. In this section, we briefly recall the key equations of the general theory [18] that will be used in the following sections. These equations will be specialized for the case of the rectangular coaxial waveguide of Fig. 1. To begin, we first write the expression for the electric field at a generic point $\mathbf{r}$ in the waveguide in the form

$$\mathbf{E}(\mathbf{r}) = -j\eta k \int_{\sigma} \overline{\mathbf{G}}_e(\mathbf{r}, \mathbf{s}', k) \cdot \mathbf{J}_\sigma\left(l'\right) dl' \tag{1}$$

where $\overline{\mathbf{G}}_e$ is the dyadic Green's function of the rectangular waveguide and $\mathbf{J}_\sigma$ is the current density on the contour σ of the inner conductor. The next step in the modal analysis is to split the current density into transversal and longitudinal components, thereby obtaining

$$\mathbf{J}_\sigma\left(l'\right) = J_t\left(l'\right)\mathbf{t}\left(l'\right) + J_z\left(l'\right)\mathbf{z}_0 \tag{2}$$

Manuscript received September 29, 1998; revised September 9, 2000. This work was supported in part by the European Union under Contract ERBFMRXCT960050.

G. Gerini is with the Physics and Electronics Laboratory, Netherlands Organisation for Applied Scientific Research (TNO–FEL), 2509 JG The Hague, The Netherlands.

M. Guglielmi is with the European Space Research and Technology Center, 2200 AG Noordwijk, The Netherlands.

Publisher Item Identifier S 0018-9480(01)03316-6.

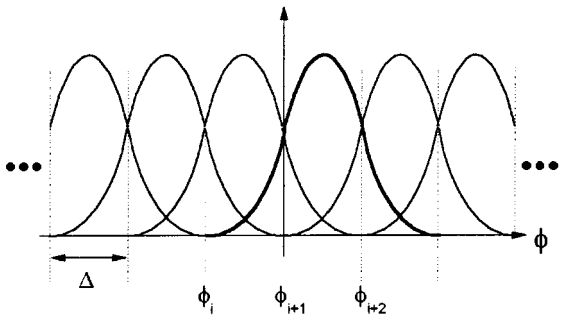

Fig. 2. Piecewise parabolic expansion functions.

where $\mathbf{t}$ is the unit vector tangential to σ. As outlined in [18], by using (2) in (1) and then imposing the boundary conditions $\mathbf{E}_t \cdot \mathbf{t} = 0$ and $E_z = 0$, respectively, on σ, we can obtain two integral equations for TE and TM modes. To solve these equations, the unknowns J_t and J_z are now represented in the form

$$J_t(l') = \sum_{n=1}^{N} b_n w_n\left(l'\right) \tag{3}$$

$$J_z\left(l'\right) = \sum_{n=1}^{N} b'_n w_n\left(l'\right) \tag{4}$$

where the expansion functions w_i are defined as

$$w_i = \begin{cases} \dfrac{2}{3\Delta^2}(\phi-\phi_i)^2, & \phi_i \le \phi \le \phi_i+\Delta \\ -\dfrac{4}{3\Delta^2}(\phi-\phi_i-3\Delta/2)^2+1, & \phi_i+\Delta \le \phi \le \phi_i+2\Delta \\ \dfrac{2}{3\Delta^2}(\phi-\phi_i-3\Delta)^2, & \phi_i+2\Delta \le \phi \le \phi_i+3\Delta \end{cases} \tag{5}$$

where ϕ is the angular coordinate, as defined in Fig. 1, Δ is the angular interval into which we have divided the inner circumference, and ϕ_i is the lower limit of the ith interval, as shown in Fig. 2. We must note that, with respect to general case outlined in [18] where two different sets of expanding functions were chosen for the TE and TM cases, we use the same set for both cases. In fact, in the particular case of the rectangular coaxial waveguide, σ has no edge points and none of its points lie on the boundary. As a consequence, the density current components do not present any singularity and their smooth behaviors can be well approximated by the same set of expanding functions (5). Furthermore, these functions can be defined on a circular domain and no poligonal approximation of the inner conductor is then required.

The last step of the modal analysis is the evaluation of the fundamental TEM mode. In this case, the field is determined as gradient of a scalar potential $\Phi(\mathbf{r})$ given by the following equation:

$$\Phi(\mathbf{r}) = \int_{\sigma} g(\mathbf{r}, \mathbf{s}')\rho_\sigma\left(l'\right) dl' \tag{6}$$

where ρ_σ represents the charge density on σ, and $g(\mathbf{r}, \mathbf{r}')$ is the same scalar Green's function for the Poisson's equation subject to the condition $g = 0$ at the boundary of the unperturbed waveguide. The unknown charge density can again be expanded with the same set of basis functions used for the TM problem.

Applying the Galerkin's procedure to the integral equations, we obtain the final eigenvalue matrix systems for the evaluation of the modal propagation constants. Spurious solutions for both TE and TM modes are generated and must be eliminated. This is easily accomplished by noting that they either correspond to the complementary problem or to modes with zero eigenvalue [18], [19]. The orthonormality condition for TE and TM modes can be assured by imposing proper conditions on the eigenvectors of the corresponding eigenvalue problems, as demonstrated in [19] and [20], respectively. The normalization condition for the TEM mode is obtained by imposing

$$\mathbf{b}''^T \cdot \mathbf{L}' \cdot \mathbf{b}'' = 1. \tag{7}$$

Here, $\mathbf{L}'$ is defined as in [18]. Since this has not been reported in the literature, we present the proof in the Appendix.

B. Coupling with Rectangular Waveguide

Once the modal structures of the noncanonical waveguides have been obtained, we can now proceed with the evaluation of the coupling integrals. In particular, for the step between the ridged rectangular waveguide and the empty rectangular waveguide, we can use the efficient procedure described in [21]. This technique, in fact, allows a very efficient evaluation of the coupling coefficients between the modes of a rectangular waveguide and those of the arbitrarily shaped waveguide with the same rectangular contour. The applicability of this approach will be extended in this section to the computation of coupling integrals between two arbitrary waveguides originating from the same basic rectangular cross section, as in the case of the ridge waveguide and rectangular coaxial waveguide in Fig. 1. Following the notation used in [21], the equations of the electric field in an arbitrary waveguide can be rewritten as follows:

$$\boldsymbol{\mathcal{E}}_q^{\mathrm{TE}}(\mathbf{r}) = \sum_{i=1}^{\infty} \mathbf{e}_i^{\mathrm{TM}}(\mathbf{r}) A_i^q + \sum_{i=1}^{\infty} \mathbf{e}_i^{\mathrm{TE}}(\mathbf{r}) B_i^q + \sum_{m=1}^{M} \mathbf{e}_m^{\mathrm{TE}}(\mathbf{r}) C_m^q \tag{8}$$

$$\boldsymbol{\mathcal{E}}_q^{\mathrm{TM}}(\mathbf{r}) = \sum_{i=1}^{\infty} \mathbf{e}_i^{\mathrm{TM}}(\mathbf{r}) D_i^q + \sum_{m=1}^{M} \mathbf{e}_m^{\mathrm{TM}}(\mathbf{r}) E_m^q \tag{9}$$

$$\boldsymbol{\mathcal{E}}_q^{\mathrm{TEM}}(\mathbf{r}) = \sum_{i=1}^{\infty} \mathbf{e}_i^{\mathrm{TM}}(\mathbf{r}) F_i^q \tag{10}$$

where $\mathbf{e}_i^{\mathrm{TE}}$ and $\mathbf{e}_i^{\mathrm{TM}}$ are the modes of the unperturbed waveguide (rectangular waveguide) and $\boldsymbol{\mathcal{E}}_q^{\mathrm{TEM}}$, $\boldsymbol{\mathcal{E}}_q^{\mathrm{TE}}$, and $\boldsymbol{\mathcal{E}}_q^{\mathrm{TM}}$ are the modes of the arbitrary waveguide (coaxial rectangular waveguide). Using this notation, we can also rewrite the expressions for the coupling integrals with the modes of the unperturbed waveguide in the form

$$\mathcal{I}_{p,q}^{\mathrm{TE,TE}} = \int_{\Omega} \mathbf{e}_p^{\mathrm{TE}}(\mathbf{r}) \cdot \boldsymbol{\mathcal{E}}_q^{\mathrm{TE}}(\mathbf{r})\, dS = B_p^q + C_p^q \tag{11}$$

$$\mathcal{I}_{p,q}^{\mathrm{TE,TM}} = \int_{\Omega} \mathbf{e}_p^{\mathrm{TE}}(\mathbf{r}) \cdot \boldsymbol{\mathcal{E}}_q^{\mathrm{TM}}(\mathbf{r})\, dS = 0 \tag{12}$$

$$\mathcal{I}_{p,q}^{\mathrm{TM,TE}} = \int_{\Omega} \mathbf{e}_p^{\mathrm{TM}}(\mathbf{r}) \cdot \boldsymbol{\mathcal{E}}_q^{\mathrm{TE}}(\mathbf{r})\, dS = A_p^q \tag{13}$$

$$\mathcal{I}_{p,q}^{\mathrm{TM,TM}} = \int_{\Omega} \mathbf{e}_p^{\mathrm{TM}}(\mathbf{r}) \cdot \boldsymbol{\mathcal{E}}_q^{\mathrm{TM}}(\mathbf{r})\, dS = D_p^q + E_p^q \tag{14}$$

$$\mathcal{I}_{p,q}^{\mathrm{TE,TEM}} = \int_{\Omega} \mathbf{e}_p^{\mathrm{TE}}(\mathbf{r}) \cdot \boldsymbol{\mathcal{E}}_q^{\mathrm{TEM}}(\mathbf{r})\, dS = 0 \tag{15}$$

$$\mathcal{I}_{p,q}^{\mathrm{TM,TEM}} = \int_{\Omega} \mathbf{e}_p^{\mathrm{TM}}(\mathbf{r}) \cdot \boldsymbol{\mathcal{E}}_q^{\mathrm{TEM}}(\mathbf{r})\, dS = F_p^q. \tag{16}$$

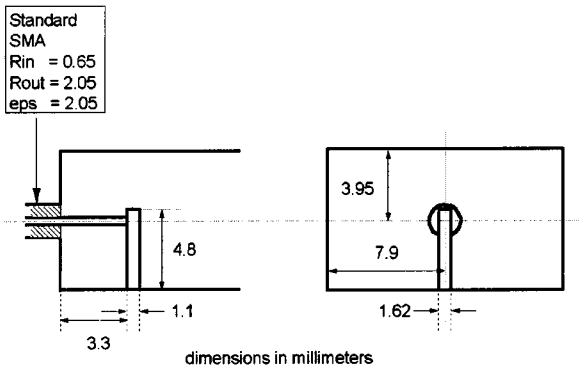

Fig. 3. Optimized coaxial transition in rectangular waveguide.

The coupling integrals between two arbitrary waveguides [(1) and (2)] can now be evaluated. For example for the TE–TE case, we have

$$\int_{\Omega} \boldsymbol{\mathcal{E}}_p^{\mathrm{TE}(1)}(\mathbf{r}) \cdot \boldsymbol{\mathcal{E}}_q^{\mathrm{TE}(2)}(\mathbf{r})\, dS = \sum_{i=1}^{M} A_i^{p(1)} A_i^{q(2)} + \sum_{i=1}^{M} B_i^{p(1)} B_i^{q(2)} + \sum_{i=1}^{M} B_i^{p(1)} C_i^{q(2)} + \sum_{i=1}^{M} C_i^{p(1)} B_i^{q(2)} + \sum_{i=1}^{M} C_i^{p(1)} C_i^{q(2)}. \tag{17}$$

Equation (17) can now be rewritten using (11) and (13), thereby obtaining

$$\int_{\Omega} \boldsymbol{\mathcal{E}}_p^{\mathrm{TE}(1)}(\mathbf{r}) \cdot \boldsymbol{\mathcal{E}}_q^{\mathrm{TE}(2)}(\mathbf{r})\, dS = \sum_{i=1}^{M} \mathcal{I}_{i,p}^{\mathrm{TM,\,TE}(1)} \mathcal{I}_{i,q}^{\mathrm{TM,\,TE}(2)} + \sum_{i=1}^{M} \mathcal{I}_{i,p}^{\mathrm{TE,\,TE}(1)} \mathcal{I}_{i,q}^{\mathrm{TE,\,TE}(2)}. \tag{18}$$

Following the same procedure, we can easily derive similar expressions for all the other cases. The upper limit M for the series running over the index i must be high enough to ensure proper convergence. In practice, however, the truncation value can be chosen to be larger or equal to the truncation value used in the computation of the admittance parameters in [16].

C. Experimental Verification of the Transition

Once all of the required *frequency-independent* calculations have been carried out, the study of the complete transition entails the solution in frequency of the banded linear system, which results from the admittance matrix representation of the cascaded waveguide sections [16]. It is important to note that this system inversion is the *only* frequency-dependent calculation that is required and that it can be carried out very efficiently, thus leading to very fast CAD tools [22]. To verify both the CAD tool described and the transition concept, we have optimized a transition from a subminiature A (SMA) connector to a WR62 waveguide. The structure obtained is shown in Fig. 3, while the measured and simulated response is shown in Fig. 4. As can be seen, very good agreement is achieved.

III. Application to Microwave Filters

As an example of application, we will now discuss the microwave filter in rectangular waveguide shown in Fig. 5. The structure has been optimized interactively using a CAD tool based on the theory described

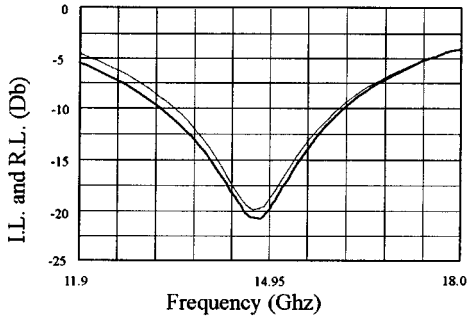

Fig. 4. Measured and simulated results for the structure in Fig. 3.

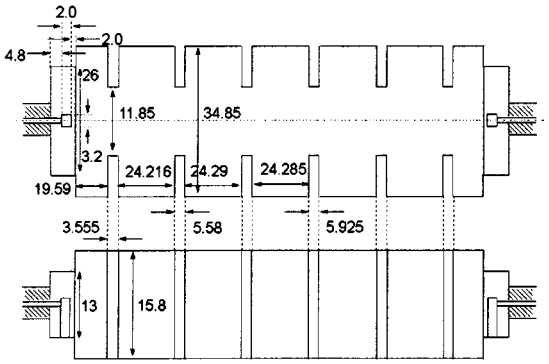

Fig. 5. Microwave filter in rectangular waveguide with integrated coaxial transition.

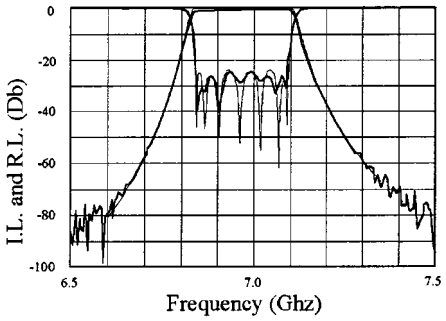

Fig. 6. Measured and simulated results for the structure in Fig. 5.

in this paper, and following the filter design procedure given in [23]. One aspect of the design procedure that deserves more attention is the proper dimensioning of the input coupling. Going back to the result shown in Fig. 4, we notice that the coaxial-to-rectangular transition exhibits a *singly tuned* resonant response. This type of response is not appropriate for filter design because it can interfere with the resonant behavior of the first cavity. This obstacle can be easily removed by decreasing the size of the rectangular waveguide at the location of the transition and adjusting the coupling to the full-size resonator with a small length of waveguide below cutoff.

The structure shown in Fig. 5 has then been manufactured using a combination of milling and spark erosion by APCO Technologies, Vevey, Switzerland. The simulated and measured in-band results are shown in Fig. 6. As we can see, very good agreement has been achieved. Note, however, that in order to obtain this result, tuning screws have been used (in the cavities only) in order to compensate for manufacturing errors. The total length of the filter with integrated transitions turns out to be essentially equal to one of the filters with standard waveguide ports, but excluding the required coaxial-to-waveguide transitions. A substantial saving in size and mass has, therefore,

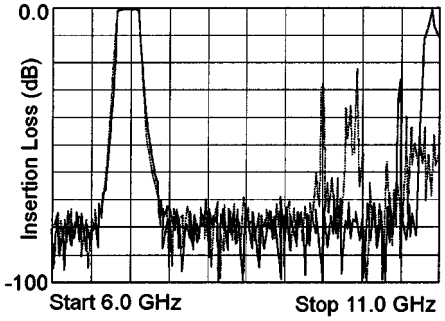

Fig. 7. Comparison of wide-band performances (dotted line indicates standard inductive filter).

been achieved. Another feature of the transition proposed that is worth mentioning is the far out-of-band response (Fig. 7). Comparing the response of the filter in Fig. 5 with the one of an inductive filter with standard coaxial-to-waveguide transitions, we can observe an increased spurious free range of about 1 GHz. This improved performance is due to the narrow-band nature of the integrated coaxial transition.

IV. Conclusions

In this paper, we have discussed a simple geometry for coaxial-to-rectangular-waveguide transitions, which can lead to a very efficient CAD for microwave filters with integrated coaxial excitation. The filter structure investigated is composed of cascaded sections of uniform waveguide so that a rigorous CAD can be carried out very efficiently. Furthermore, the integration of the transition in the filter design results in an improved out-of-band response and in significant saving in size and mass with respect to standard inductive filters in rectangular waveguide. The key elements of the CAD tool developed have been discussed, and measured results have also been presented. Very good agreement between measured and simulated results has been achieved, thus validating at the same time both the filter structure and the theory developed.

Appendix
Normalization Condition for Arbitrary TEM Modes

The normalization condition for the TEM mode is

$$\iint_S \nabla\phi(x,\,y)\cdot\nabla\phi(x,\,y)\,dS = 1 \tag{19}$$

where S is the cross section of the rectangular coaxial waveguide of Fig. 1. Using the following vector identity:

$$\nabla\cdot(\psi\mathbf{A}) = \mathbf{A}\cdot\nabla\psi + \psi\nabla\cdot\mathbf{A} \tag{20}$$

(19) becomes

$$\iint_S \nabla\cdot\Big(\phi(x,\,y)\nabla\phi(x,\,y)\Big)\,dx\,dy - \iint_S \phi(x,\,y)\nabla^2\phi(x,\,y)\,dx\,dy = 1. \tag{21}$$

Applying the divergence theorem in two dimensions to the first term of (21), we can transform it into the following contour integral:

$$\oint_{\gamma_S} (\phi\nabla\phi)\cdot\hat{n}\,d\ell \tag{22}$$

where $\gamma_S = \gamma_0 + \gamma_1$ is the contour of the rectangular coaxial waveguide, γ_0 is the outer rectangular contour, and γ_1 is the inner circular conductor. Furthermore, the second term of (21) is identically zero because the potential of the TEM mode satisfies the following equation:

$$\nabla^2\phi = 0, \qquad \text{on } S. \tag{23}$$

Equation (21) can now be rewritten as follows:

$$\oint_{\gamma_S} (\phi\nabla\phi)\cdot\hat{n}\,d\ell = \oint_{\gamma_0} (\phi\nabla\phi)\cdot\widehat{n_0}\,d\ell + \oint_{\gamma_1} (\phi\nabla\phi)\cdot\widehat{n_1}\,d\ell = 1. \tag{24}$$

Imposing, for the solution of (23), the following boundary conditions:

$$\phi = 0, \qquad \text{on } \gamma_0 \tag{25}$$

$$\phi = 1, \qquad \text{on } \gamma_1 \tag{26}$$

we can obtain from (24)

$$-\oint_{\gamma_1} \mathbf{D}\cdot\widehat{n_1}\,d\ell = \oint_{\gamma_1} D_n\,d\ell = 1 \tag{27}$$

where we used the identity $-\nabla\phi = \mathbf{D}$. Finally, considering the boundary condition $D_n = \rho$ on γ_1, (27) becomes

$$\oint_{\gamma_1} \rho\,d\ell = \sum_{n=1}^{N} b_n'' \oint_{\gamma_1} w_n(\ell)\,d\ell = 1 \tag{28}$$

which can be rewritten in the following matrix form:

$$\mathbf{b}''^{T}\cdot\mathbf{L}'\cdot\mathbf{b}'' = 1 \tag{29}$$

where $\mathbf{L}'$ is defined as in [18]. This is the normalization condition (7) that must be imposed on $\mathbf{b}''$ in order to guarantee the normalization of the TEM mode.

References

[1] M. J. Al-Hakkak, "Experimental investigation of the input-impedance characteristics of an antenna in a rectangular waveguide," *Electron. Lett.*, vol. 5, no. 21, pp. 513–514, Oct. 1969.
[2] A. G. Williamson and D. V. Otto, "Coaxially fed hollow cylindrical monopole in a rectangular waveguide," *Electron. Lett.*, vol. 9, no. 10, pp. 218–220, May 1973.
[3] A. G. Williamson, "Coaxially fed hollow probe in a rectangular waveguide," *Proc. Inst. Elect. Eng.*, pt. H, vol. 132, pp. 272–285, 1985.
[4] A. G. Williamson and D. V. Otto, "Cylindrical antenna in a rectangular waveguide driven from a coaxial line," *Electron. Lett.*, vol. 8, no. 22, pp. 545–547, Nov. 1972.
[5] A. G. Williamson, "Equivalent circuit for a coaxial-line rectangular-waveguide junction," *Proc. Inst. Elect. Eng.*, pt. H, vol. 129, pp. 262–270, 1982.
[6] ——, "Analysis and modeling of a coaxial-line rectangular-waveguide junction," *Proc. Inst. Elect. Eng.*, vol. 132, pp. 272–285, 1985.
[7] ——, "Radial-line coaxial-line junctions: Analysis and equivalent circuits," *Int. J. Electron.*, vol. 58, pp. 91–104, 1985.
[8] Y. Leviatan, P. G. Li, A. T. Adams, and J. Perini, "Single-post inductive obstacle in a rectangular waveguide," *IEEE Trans. Microwave Theory Tech.*, vol. MTT-31, pp. 806–812, Oct. 1983.
[9] Y. Leviatan, D. Shau, and A. T. Adams, "Numerical study of the current distribution on a post in a rectangular waveguide," *IEEE Trans. Microwave Theory Tech.*, vol. MTT-32, pp. 1411–1415, Oct. 1984.
[10] J. M. Jarem, "A multifilament method-of-moments solution for the input impedance of a probe-excited semi-infinite waveguide," *IEEE Trans. Microwave Theory Tech.*, vol. MTT-35, pp. 14–19, Jan. 1987.
[11] D. V. Otto, "The admittance of cylindrical antennas driven from a coaxial line," *Radio Sci.*, vol. 2, pp. 1031–1042, Sept. 1967.

[12] L.-W. Li, P.-S. Kooi, M.-S. Leong, T.-S. Yeo, and S.-L. Ho, "Input impedance of a probe-excited semi-infinite rectangular waveguide with arbitrary multilayered loads: Part I—Dyadic Green's functions," *IEEE Trans. Microwave Theory Tech.*, vol. 43, no. 7, pp. 1559–1566, July 1995.

[13] ——, "Input impedance of a probe-excited semi-infinite rectangular waveguide with arbitrary multilayered loads: Part II—A full-wave analysis," *IEEE Trans. Microwave Theory Tech.*, vol. 45, no. 3, pp. 321–329, Mar. 1997.

[14] J. Liang, H. Chang, and K. A. Zaki, "Coaxial probe modeling in waveguide and cavities," *IEEE Trans. Microwave Theory Tech.*, vol. 40, pp. 2172–2180, Dec. 1992.

[15] M. Saad, "A more accurate analysis and design of coaxial-to-rectangular waveguide end launcher," *IEEE Trans. Microwave Theory Tech.*, vol. 38, pp. 129–134, Feb. 1990.

[16] A. Alvarez and M. Guglielmi, "New simple procedure for the computation of the multimode admittance matrix of arbitrary waveguide junctions," in *IEEE MTT-S Int. Microwave Symp. Dig.*, Orlando, FL, May 1995, pp. 1415–1418.

[17] R. E. Collin, *Foundations for Microwave Engineering*, 2nd ed. New York: McGraw-Hill, 1992.

[18] G. Conciauro, M. Bressan, and C. Zuffada, "Waveguide modes via an integral equation leading to a linear matrix eigenvalue problem," *IEEE Trans. Microwave Theory Tech.*, vol. MTT-32, pp. 1495–1504, Nov. 1984.

[19] P. Arcioni, M. Bressan, G. Conciauro, and L. Perregrini, "Wide-band modeling of arbitrarily shaped E-plane waveguide components by the boundary integral-resonant mode expansion method," *IEEE Trans. Microwave Theory Tech.*, vol. 44, pp. 2083–2092, Nov. 1996.

[20] P. Arcioni, M. Bressan, and G. Conciauro, "Wide-band analysis of planar waveguide circuits," *Alta Freq.*, vol. LVII-N.5, pp. 217–226, June 1988.

[21] P. Arcioni, "Fast evaluation of modal coupling coefficients of waveguide step discontinuities," *IEEE Microwave Guided Wave Lett.*, vol. 6, pp. 232–234, June 1996.

[22] V. E. Boria, G. Gerini, and M. Guglielmi, "An efficient inversion technique for banded linear systems," in *IEEE MTT-S Int. Microwave Symp. Dig.*, 1997, pp. 1567–1570.

[23] M. Guglielmi, "Simple CAD procedure for microwave filter and multiplexers," *IEEE Trans. Microwave Theory Tech.*, vol. 42, no. 7, pp. 1347–1352, July 1994.

Single-Ended HEMT Multiplier Design Using Reflector Networks

Donald G. Thomas, Jr. and G. R. Branner

***Abstract*—Microwave and RF frequency multipliers are employed in a large number of communications, radar, civilian, and military systems. This paper presents the development of active doublers operating in S and C frequency bands. These devices are unique in that high electron-mobility transistors (Fujitsu FHX35LG) are employed in an unbalanced configuration utilizing "reflector" networks simultaneously on the input and output to reflect the second harmonic signal into the gate of the device and the fundamental signal into the drain simultaneously at appropriate phase angles to optimize performance. Measured and simulated results are presented on over 20 multiplier designs to verify the design philosophy. Conversion gains of approximately 7 dB are presented for narrow-band designs (5% bandwidth), 5 dB for medium-bandwidth designs (15%), and 4 dB for wide-bandwidth designs (35%). The fundamental and third harmonic rejection is approximately 40 dBc for the narrow-band designs and greater than 50 dBc for the medium and wide-band designs.**

I. Introduction

Numerous techniques exist for realization of frequency multipliers using passive or active devices. While high electron-mobility transistors (HEMTs) are traditionally employed in high-gain or low-noise amplifiers, less information is available on their use in multiplier applications. This is in marked contrast with multiplier realizations employing bipolar and FET devices.

The basic configuration of Fig. 1 is employed in the frequency multiplier realization of this paper. The input network is designed to pass the fundamental frequency component to the gate of the HEMT (common-source configuration), while suppressing higher harmonic components. Likewise, the output network suppresses the fundamental and other undesired harmonics, while passing the desired harmonic. The frequency multiplier reflector network design philosophy implemented in this paper is applied to frequency doublers utilizing a fundamental frequency of 3 GHz as a vehicle.

As mentioned previously, a primary objective of the output and input networks is to suppress the fundamental and second harmonics, respectively. In the process of suppressing the undesired signals, it appears that not a great amount of attention has been focused on the concept of reflecting signals back into the device from the input and output networks, although it has been utilized occasionally as pointed out below. The device nonlinearities cause harmonics and the fundamental to mix with other frequency components and either enhance or degrade the signal at the desired output harmonic. Therefore, it is important for the reflected signal to be phased properly to interfere constructively with the desired harmonic. Thus, in concert with their primary filtering and matching functions, the input and output networks of Fig. 1 can be designed in such a way that they are reflector networks meeting the above criteria.

Due to the complexity of calculating the actual effects of the reflector networks, the published literature to date on this topic is sparse [1]–[4]. Using reflector networks as a design tool for frequency doublers, Hirota [1] gave simulated data on the effects of a reflector network on the output of a GaAsFET versus conversion gain, and realized

Manuscript received November 24, 1998; revised September 18, 2000.

D. G. Thomas, Jr. is with Panasonic–MCUSA, Peachtree City, GA 30269 USA (e-mail: thomasd@Panasonic-mcusa.com).

G. R. Branner is with the Department of Electrical and Computer Engineering, University of California at Davis, Davis, CA 95616 USA.

Publisher Item Identifier S 0018-9480(01)03317-8.